Quantity Distribution Search using Sparse Representation Generated with Kernel-based Regression

Akinori Asahara and Hideki Hayashi
Center for Technology Innovation-System Engineering, Hitachi Ltd., Kokubunji-shi, Tokyo, Japan

Keywords: Database, Multi-dimensional Array Data, GIS, Regression.

Abstract: The number of records representing a quantity distribution (e.g. temperature and rainfall) requires an extreme amount of overhead to manage the data. We propose a method using a subset of records against the problem. The proposed method involves an approximation derived with kernel ridge regression in advance to determine the minimal dataset to be input into database systems. As an advantage of the proposed method, processes to reconstruct the original dataset can be completely implemented with Structured Query Language, which is used for relational database systems. Thus users can analyze easily the quantity distribution. From the results of experiments using digitized elevation map data, we confirmed that the proposed method can reduce the number of data to less than 1/10 of the original number if the acceptable error was set to 125 m.

1 INTRODUCTION

Meteorological observation data, such as rainfall and temperature(Christensen et al., 2010)(Hofstra et al., 2009)(the European Climate Assessment & Dataset project team, 2016), were generally intended for professional users (e.g. meteorologists). However, more "casual" users (e.g. city government officers and marketing analyzers) are now requiring such data to improve their work. For example, imagine that several stores' sales figures are simultaneously dropping. A marketer will assume many hypotheses for and test them statistically. He/she might find a fact that it was raining around the stores when their sales figures dropped. In this case, conditions effective for the sales figure drop were discovered by trial-and-error processes. Such a process to find crucial conditions is called "drill down."

We often face a serious problem when conducting a drill-down process: the dataset is too large to handle. The number of records representing a quantity distribution (e.g. temperature and rainfall) is often very large. Assume a 100 $\times$ 100 km region described with small cells, the edges of which are 250 m, and a snap shot taken hourly. To store snapshot history of 10 years, 14 billion cells must be handled. Coverages and sampling rate of such data is enhanced - the number of records might be over 3360 billion for 200 $\times$ 200 km minutely sampled data. It generally requires an extreme amount of time to retrieve the required information from such a huge dataset. For accelerating retrieval, duplicated storages are used to parallelize access to the data; however, the multiple storages increase storage system cost.

To reduce the cost, we propose a method using a small subset of data (called "sparse representation") to construct an approximation function stored in the DB. The approximation function is derived with an iteration of kernel-based regression. The iteration is carried out until the errors of an approximation function are less than a preset threshold. Hence, the original dataset can be reconstructed with the small subset of data without errors larger than the preset threshold. The reconstruction process can be completely implemented with Structured Query Language (SQL) supported by general relational database systems. Moreover, with digitized elevation map (DEM) data, we confirmed that the proposed method can decrease the number of data to less than 1/10 of the original one.

2 RELATED WORKS

2.1 Problem Setting

A grid-based representation (sometimes they are called 'raster data') is frequently used for various types of data, such as remote sensing results, physical simulations like a flood simulations(Bates and

Asahara, A. and Hayashi, H.
Quantity Distribution Search using Sparse Representation Generated with Kernel-based Regression.
DOI: 10.5220/0006316402090216
In *Proceedings of the 3rd International Conference on Geographical Information Systems Theory, Applications and Management (GISTAM 2017)*, pages 209-216
ISBN: 978-989-758-252-3

Table 1: Schema of a distribution data.

Name	Description	Name	Description
id	ID of records	y	y coordinate value
did	ID of distributions	t	time (hour)
x	x coordinate value	v	the quantity

De Roo, 2000), and so on(Park et al., 2005)(Hofstra et al., 2009)(the European Climate Assessment & Dataset project team, 2016). Many algorithms to generate grid data from a point dataset have also been proposed (Silverman, 1986) (Seaman and Powell, 1996)(Asahara et al., 2015). This implies that such grid data are useful for various use cases.

Table 1 lists items of a table-managing grid data modeling a quantity distribution. Every distribution, having an identifier of a distribution (denoted as `did`), consists of multiple records. The records have location data (denoted as `x,y`), time data (denoted as `t`) and the quantity value denoted as `v`.

Using spatio-temporal-indexing technologies, we can quickly retrieve the quantity data any place any time. A query, for example, is following.

```
select did from distribution where
 (x between 10 and 20)
 and (y between 10 and 20)
 and (t between 10 and 15)
 and (v > 100.0)
```

The result of this query is a list of `did`s, the `v` of which in a square $10 < x < 20$ and $10 < y < 20$ was more than 100.0 in between 10:00 and 15:00. A usecase of the query is a hypothesis test of "the sales figures of a store in $10 < x < 20$ and $10 < y < 20$ was quite high during heavy rain (more than 100mm)." The query is very simple. The overhead of managing relational database systems (RDBMS), however, is extremely large due to the huge number of records in the database (e.g. 14 billion records as discussed above).

2.2 Related Works

Many indexing technologies for spatio-temporal point data have been proposed (Koubarakis et al., 2003)(Hayashi et al., 2015)(Haynes et al., 2015)(Theodoridis et al., 1998). These technologies are applicable to the quantity distribution datasets because the data can be handled as point data. However, the number of records makes problems of the storage cost as discussed above. Thus methods to reduce DB records without loss of accuracy are required from the aspect of costs.

Additionally many indexing techniques for raster data are proposed(Zhang et al., 2010)(Pajarola and Widmayer, 1996) and implemented(Shyu et al., 2007). The scientific array databases(Oracle, 2014) moreover are produced to handle such grid datasets. SciDB(Stonebraker et al., 2013) and Rasdaman(Baumann et al., 1999) are well-known software to manage array data. For such systems, SQL Multidimensional Array(International Standard Organization,) for queries to array data was standarized. Most of them are based on the raster boundaries and its hierarchical structure, such as R-trees and quad trees but data themselves are not reduced. Note that these methods and a record reduction might be used together to create a synergy effect. For example, the reduced records can be retlieved with a spatio-temporal indexing technology.

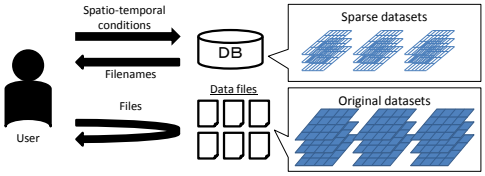

Figure 1: Sparse-data-based system.

2.3 Approach

As a solution to the problem, our method reduces the number of records without loss of information. Figure 1 illustrates an overview of a sparse-data-based system. A user of this system requests the database (labeled as DB in the figure) for distributions satisfying a condition. The user obtains filenames corresponding to the `did` as "candidates". The user can thus find distribution data files (e.g. NetCDF (Open Geospatial Consortium, 2010) files). The user finally obtains the desired distribution data files. Note the DB is not used for finding the final results. The DB manages a rough distribution for finding candidates. Therefore, the number of records in the database can be smaller than that of the original records. The user will require various queries without programming. SQL, which is one of the most frequently used languages, is useful for such users. Thus, the process to request the database should be completely written in SQL, that is, the database should be implemented with a RDBMS.

Another point is precision. Generally, most measurements include errors due to observation. This fact suggests that the users of the system can accept small errors. Although some users might require the most accurate information, the original dataset should be accessible. Figure 2 illustrates the mechanism to retrieve the original data. The vertical axis is v and the horizontal axis is x, in the illustration. The solid curve represents distribution of the original dataset. The white circle shown in the center of the graph represents the roughly estimated v at x_i and the square

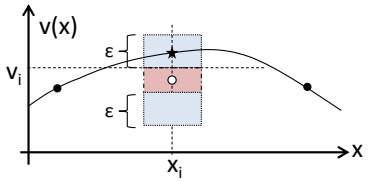

Figure 2: Query with error ε.

colored by red shows the range of a query (data in the red region should be retrived). Because the estimated value is not accurate, the actual value represented by the black star is out of the red region. However, bacause the error is less than ε, distance between the white circle and the black star is less than ε. Thus the actual value can be obtained if the query region was set as the red region plus the blue region which represents the range of which is added by ε. As shown in this example, even if the data have an error $\pm\varepsilon$, the query condition with $\pm\varepsilon$ hits all possible distributions. The result might include unnecessary distributions, though they can be removed after fetching the original datasets. Therefore, the database can accept a small error less than a preset threshold denoted as ε.

2.4 Contribution

In summary of the last section, the distribution data in the database should be fewer than the original dataset. Additionally, a query to obtain one of the distribution data should be written in SQL for usability. Alternatively the distribution data may be imprecise. Thus, a small dataset having information to reconstruct the original dataset should be managed in a RDBMS.

One of the naive approaches to reduce the number of data is random sampling, which involves randomly removing some of the data, so precision cannot be controlled. Another naive approach involves using the averages of multiple data. However, precisions of sparse representations using such methods are quite low. Generally the reconstruction with fewer information will be difficult, therefore the records in RDBMS cannot be recuded so much to keep information enough to the reconstrucion.

We therefore propose a method using a sparse representation generated with kernel regressions(John Shawe-Taylor, 2004). A kernel regression, which is defined as a regression using a kernel trick, is commonly used for prediction, interpolation, and so on. Inputs of a kernel regression are point-value pairs. A kernel regression constructs a non-linear function to predict values at such points.The basic concept of the kernel trick is that an imaginary non-linear transformation is assumed to find a linear regression function. The formula of a linear regression function can be changed to another formula using only similarities between input data. Therefore, all that needs to be defined is the similarity formula, which is called a kernel function. The regression function is very precise; thus, the original dataset can be accurately reconstructed. Therefore, a highly sparse representation of a quantity distribution can be derived using a kernel regression.

3 SPARSE REPRESENTATION GENERATED WITH KERNEL REGRESSION

3.1 Kernel Ridge Regression

Many kernel regressions have been proposed such as a support vector regression (SVR) (Vapnik et al., 1997). The proposed method uses a kernel ridge regression, which is equivalent to Kriging (Kbiob, 1951)(Press et al., 2007) used for geostatistics. A ridge regression is a linear regression method based on "least square mean errors". The formula of the ridge regression is non-linearized with the kernel trick to obtain the kernel ridge regression. The regression result denoted as $v(x)$ is written as follows.

$$v(x) = \begin{pmatrix} v_1 & v_2 & \cdots \end{pmatrix} (G+\sigma I)^{-1} \begin{pmatrix} \kappa(x_1,x) \\ \kappa(x_2,x) \\ \vdots \end{pmatrix} \quad (1)$$

where I is a unit matrix, σ is a parameter, and G is called 'Gram matrix.' G is defined as

$$G = \begin{pmatrix} \kappa(x_1,x_1) & \kappa(x_1,x_2) & \cdots \\ \kappa(x_2,x_1) & \kappa(x_2,x_2) & \cdots \\ \vdots & \vdots & \ddots \end{pmatrix}. \quad (2)$$

The $\kappa(\cdot,\cdot)$ is a kernel function to evaluate the similarity of two data. Note that $v(x_i)$ always equals v_i (i.e. the product of G^{-1} and $(\kappa(x_1,x_2),\kappa(x_2,x_2),\cdots)$ is $(0,1,0,\cdots)$) when $\sigma = 0$. Thus, $v(x)$ with $\sigma = 0$ can completely reconstruct the original distribution if all of the original data are involved by $v(x)$. This ensures the lower bound of the error as 0. Therefore, any threshold ε can be acceptable.

3.2 Sparse Representation Generation

The algorithm of our proposed method to generate a sparse representation dataset is shown in Algorithm 1. The initial dataset is set to a dataset including only the point at the origin (0,0) for simplifying the algorithm. It can be set to another small dataset though the choice

Algorithm 1: Naive sparse representaion generation.

Data: Original dataset $\{x_i\}$, preset threshold ε and parameter θ
Result: sparse representation $\{x'_i\}$ and weights $\{w_i\}$
begin
  initialize sparse dataset $\{x'_i\}$ from $\{x_i\}$
  initialize G^{-1} with formula (2) using $\{x'_i\}$
  while *the number of* $\{x'_i\} \neq$ *the number of* $\{x_i\}$ **do**
    find the maximal-error point out from $\{x_i\}$ with formula (1) using G^{-1}
    (point x_m, error e) $\leftarrow$ the maximal-error point
    if $e \leq \varepsilon$ **then**
      end this loop
    Append x_m to $\{x'_i\}$
    update G^{-1} with formula (2) using $\{x'_i\}$
  return $\{x'_i\}$ *and* $\{w_i\}$

does not make significant effect because much more data will be added. An iteration is carried out at the next step. If maximal error of the generated function is lower than the preset threshold ε, the iteration should be finished to output the dataset as the sparse representation. If the maximal error is even more than ε, another data needs to be added to improve accuracy. The data with the maximal error (hereafter, called the max-error point) is selected as the data to be added because it lowers the maximal error. The maximal error in the next iteration is thus automatically changed, so another data will be selected to be added in the next iteration. The kernel ridge regression result completely reproduces the input data as mentioned above. The maximal error will be 0 after adding all the original data to the sparse representation. Therefore, the sparse representation is equivalent to the original dataset in the worst case.

An inverse matrix of Gram matrix G^{-1} is calculated in the iteration. The calculation takes much time because the computational complexity is $o(n^3)$ (n is the dimension of G, that is, the number of data). The recurrence formula is thus used for accelerating the calculation. The formula of a Gram matrix using n data, G_n, is written as

$$G_{n+1} = \begin{pmatrix} G_n & c_{n+1} \\ c_{n+1}^T & \kappa(x_{n+1}, x_{n+1}) \end{pmatrix}, c_n = \begin{pmatrix} \kappa(x_1, x_n) \\ \vdots \end{pmatrix}. \tag{3}$$

By using the formula for the inverse of a block matrix

$$\begin{pmatrix} A & B \\ C & D \end{pmatrix}^{-1} = \begin{pmatrix} A^{-1} + A^{-1}BECA^{-1} & -A^{-1}BE \\ -ECA^{-1} & E \end{pmatrix} \tag{4}$$

$$E = (D - CA^{-1}B)^{-1} \tag{5}$$

the following formula is obtained.

$$G_{n+1}^{-1} = \frac{1}{s}\begin{pmatrix} sG_n^{-1} + VV^t & -V \\ -V^t & 1 \end{pmatrix}, \tag{6}$$

where

$$s = \kappa(x_{n+1}, x_{n+1}) - c_{n+1}^T G_n^{-1} c_{n+1} \tag{7}$$

$$V = G_n^{-1} c_{n+1}. \tag{8}$$

The algorithm is quite similar to the Douglas-Peucker algorithm (David and Thomas, 1973) known as a simplification algorithm for a polyline. The Douglas-Peucker algorithm has an issue regarding the computation time in finding the furthest point (Hershberger and Snoeyink, 1994). Similarly, the algorithm of the proposed method to generate a sparse representation also has an issue regarding processing speed in finding the maximal-error point. An error of a point, which is defined as $|v(x_i) - x_i|$, includes the evaluation of $v(x)$. Calculation time for this evaluation will be huge due to the number of original data because it is convolution of sparse representation for all data of the original dataset. Accordingly the convolution should be carried out on a small region to reduce calculation time. In addition, doubly evaluated $v(x)$ should be sorted out, that is, $v(x)$ values calculated in the former iteration are suitable for the later iteration until the values are changed.

3.3 Kernel Functions

Various kernel functions are already known such as Gaussian kernel and polynomial kernel function, which affect an infinite region. The algorithm of the proposed method, however, has a problem caused by the huge number of the original data if the kernel function widely affects $v(x)$. So the polynomial kernel function is suitable for the proposed method, described as

$$\kappa(x_i, x_j) = \begin{cases} \left(1 - \frac{|x_i - x_j|^2}{\theta}\right)^d & (\frac{|x_i - x_j|}{\theta} < 1) \\ 0 & (\frac{|x_i - x_j|}{\theta} > 1) \end{cases}, \tag{9}$$

where θ is a parameter to be set manually. The function is an exponent of a quadratic function normally used in density estimation. The function, called exponential circular kernel (ECK) hereafter, is applicable to the kernel ridge regression.

The effect of the ECK is limited in a circle the radius of which is θ. Hence, the calculation of $v(x)$ is shortened.

$$v(x) = \sum_{|x_i - x| < \theta} w_i \kappa(x_i, x) \tag{10}$$

Algorithm 2: Sparse representaion generation.

Data: Original dataset $\{x_i\}$, preset threshold ε and parameter θ
Result: sparse representation $\{x'_i\}$ and weights $\{w_i\}$

1 **begin**
2 initialize sparse dataset $\{x'_i\}$ from $\{x_i\}$
3 initialize G^{-1} with formula (2) using $\{x'_i\}$
4 initialize $\{w_i\}$ with formula (11) using G^{-1} and $\{x'_i\}$
5 initialize heap H for $\{x_i\}$ with formula (10) using ($\{x'_i\}$,$\{w_i\}$)
6 **while** *the number of* $\{x'_i\} \neq$ *the number of* $\{x_i\}$ **do**
7 (point x_m, error e) $\leftarrow$ pull the maximal-error point out from H
8 **if** $e \leq \varepsilon$ **then**
9 end this loop
10 Append x_m to $\{x'_i\}$
11 incrementally update of G^{-1} and $\{w_i\}$ with formula (6)
12 **for** *each* x *with* $|x - x_m| < \theta$ **do**
13 update error $|x - v(x)|$ of x in H with formula (10) using ($\{x'_i\}$, $\{w_i\}$)
14 maintain heap structure of H for x
15 **return** $\{x'_i\}$ *and* $\{w_i\}$

where w_i is defined as

$$w_i = \sum_{|x_i - x_j| < \theta} v_j G^{-1}_{i,j}. \quad (11)$$

Parameter θ shown in the ECK accordingly indicates the distance in which the quantity of the distribution does not change much, that is, the range of blur. d indicates the sharpness of the distribution. The parameters should be tuned for the distribution with parameter tuning methods such as cross validations.

Furthermore, the step to find the maximal-error point can be accelerated with ECK, as shown in Algorithm 2. The code shows a function to generate a sparse representation of the given dataset denoted by the original dataset $\{x_i\}$. A minimal dataset $\{x'_i\}$ is initially set to be very small and the inverse matrix of the Gram matrix is calculated only once at the initialization. The $\{x'_i\}$ is enlarged during the iteration and G^{-1} is incrementally updated with formula (6). When a new data is added, $v(x)$ only at the θ-radius region around the data is changed. Therefore, for the other $v(x)$s, the calculation results at the former iterations are re-usable. A well-known heap-sort algorithm is suitable for finding the maximal-error point. Namely, all pairs of errors $|y_i - v(x_i)|$ and data x are initially calculated and managed in a max heap H. The maintenance of H (e.g. the loop at line number 12 in Algorithm 2) is limited around the maximal-error point due to the ECK. The maximal-error point can be easily removed from the heap because the top of the heap is the maximal-error point. After adding the maximal-error point to the sparse representation, the $|y_i - v(x_i)|$ to be updated are calculated and reflected to the data in the heap. The heap structure can be maintained in $O(n \log n)$ runtime, so the process to find the maximal-error point is quite fast.

Thus, the sparse representations `did`, `x`, `y`, `t`, and `w` have to be stored in a relational database. The reconstruction can be implemented with SQL as follows.

```
select sid, sum(w* pow(1.0
 -dist([{x0,y0}],{x,y})/[theta]),[d])
from distribution
where dist([{x0,y0}],{x,y}) < [theta]
 group by sid
```

where `dist(·,·)` is a function to calculate the Euclidian distance between two points and [ ] indicates the query condition given by the user.

4 EXPERIMENTS

To evaluate how small a sparse representation dataset generated with the algorithm of the proposed method is, we conducted an experiment using actual quantity-distribution data.

The dataset, summarized in Table 2, contains the DEM data of Shizuoka prefecture of Japan (the ID of this region is 5238)(Ministry of Land, Infrastructure, Transport and Turism, 2014). The region was split into 320 $\times$ 320 grids to represent the distribution of the ground surface height, where the grid size was around 250 m. The dataset consisted of 102,400 records, including the invalid data on the height of the ocean. After removing the ocean data, there were 74,663 records - this was the baseline. The computer used for the experiment had an Intel Corei-7 3770K 3.5-GHz CPU and 16-GB RAM. The sparse representation generation algorithm was implemented with Java, and JDK 1.8.0 update 31 on OS Windows 7 was used as the environment to run it.

To exhibit how the parameter ε works, two parameter settings were tested in the experiment. As the first setting, ε was set to 125 m; θ was set to 5 (1250 m); degree of the ECK was $d = 2$. The calculation to generate the sparse representation took 383.8 s. The threshold was set to 250 m; θ was set to 5 (1250 m); and degree of the ECK $d = 2$. The calculation time was 74.9 seconds. The results indicate that the threshold setting is crucial for performance.

The datasets were imported into PostgreSQL 9.2 database and a multicolumn b-tree index to x and y

Table 2: Overview of the DEM dataset.

Name	description
Size	3.8MB on RDBMS
# of records	102,400 records 74,663 records for ground surface
Region ID	5238 around Shizuoka Pref.

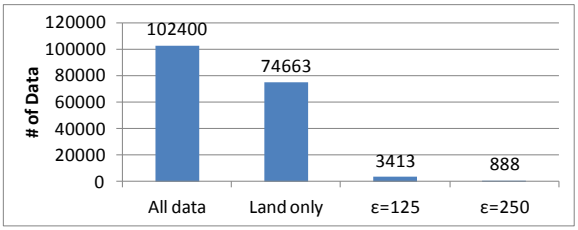

Figure 3: The number of records.

is generated to evaluate the performance to manage the original data. Figure 3 plots the number of the sparse representations and that of the original data. The table data size of the original dataset consisting of 74,663 records was 3.8MB and the index size was 3.0MB. The sparse representation with ε =125m consists of 2,898 records (3.9% of Land only data). The table data size was 152KB; index datasize was 168KB. The sparse representation ε =250m consists of 1,133 records (1.5%); the table data size of PostgreSQL was 64KB; index datasize was 64KB.

The original dataset reconstruction was also carried out for the same dataset to confirm the quality. For the sparse dataset of $\varepsilon = 125$ and $\varepsilon = 250$, a reconstruction query of one grid was finished in 12 ms. The query for the record to the original dataset finished in 11 ms. This shows data reconstruction implemented by SQL is not slow in obtaining a reconstructed dataset. Figures 4, 5(a), and (b) respectively present the original distribution, images reconstructed with sparse representation with $\varepsilon = 125$ m, and that with sparse representation with $\varepsilon = 250$ m. They are quite similar but the details are not. Figures 6 and 7 compare close-up images of the regions marked with red squares in Figures. 4 and 5, respectively. The original dataset had small irregularities, which were smoothed in the sparse representations. The sparse representation with 250 m was rougher than that with 125 m. In addition to the conditions, $\varepsilon = 375$ and $\varepsilon = 500$ were also tested; the number of records was

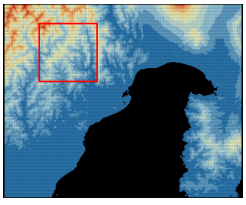

Figure 4: Original dataset.

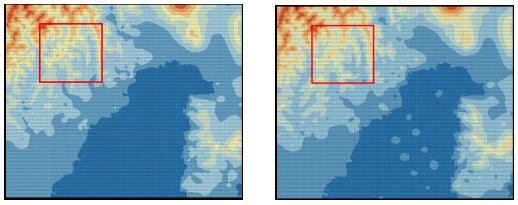

(a) 125m (b) 250m

Figure 5: Sparse representations.

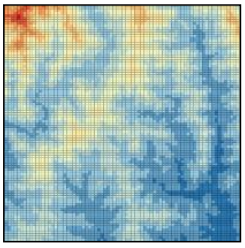

Figure 6: Close-up image of the original dataset.

293 and 148; the processing time were 20.4 s and 10.3 s, respectively. The results shows that the accuracy and the speed of the algorithm of the proposed method sensitively depend on ε. Therefore, ε should be used to precisely reconstruct the original dataset.

Figures 8 illustrate the sparse representation and close-up image. The red triangles are the location of the sparse dataset. Fewer data were on a flat region and more data were on irregular regions. Many data were put along the coastline because elevations of the coastline indicate extreme gaps in land and sea levels. This tendency suggests that the proposed method works well to remove unnecessary flat data.

Additionally the parameters used in the proposed method are changed to clarify the effects. Figure 9 plots the number of records by various θ (ε was set to 250). When θ is 10, the number of records was largest. Because θ gives the range of the effect by the ECK, more records were needed for covering all regions when θ was small. Figure 9 plots the precisions for each θ. The vertical axis of the graph represents the averaged errors with the sparse representations. More sparse representation was expected to give accurate results though the larger θ gave precise results.

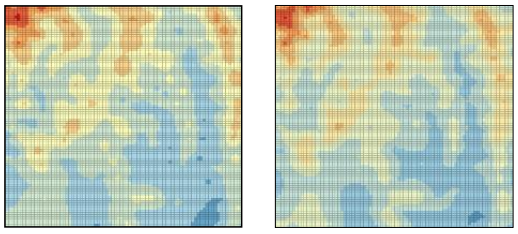

(a) 125m (b) 250m

Figure 7: Close-up images of sparse representations.

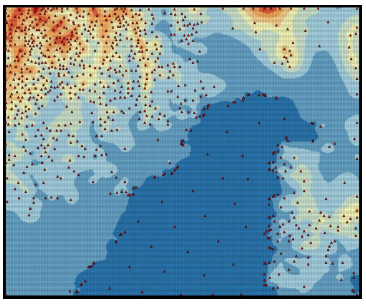

(a) overview

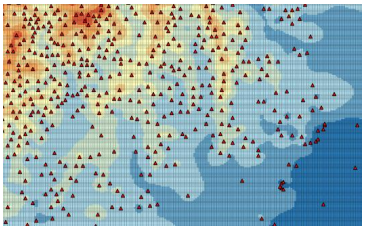

(b) close-up image

Figure 8: Data of sparse representation.

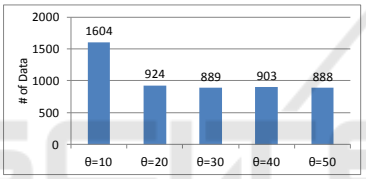

Figure 9: The number of records by θs.

The proposed algorithm is based on the max error, so sparseness of the sparse representation is not correlated to the accuracy. Figure 11 plots the processing times for each θs. The fastest setting was $\theta = 20$. Generally if θ is smaller, more records are required as disscussed above. Thus, when a small θ is used, the processing time is longer. However, θ is the range of the effect by the ECK also. That is, the region to be calculated might be small when a small θ is used. The fact implies that the processing time is shorter. These two factors are balanced at θ=20 in the case.

Moreover graphs shown in Figure 12 plot the number of records for each d of ECK. When $\theta = 30$, $d = 3$ gave the minimal number of records; $d = 5$ gave the minimal number of records when $\theta = 50$. Generally large d gives a sharp ECK. So d should be tuned

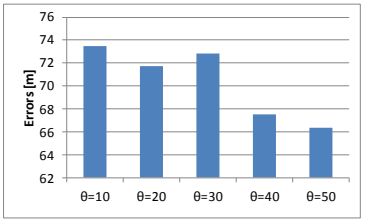

Figure 10: The precisions by θs.

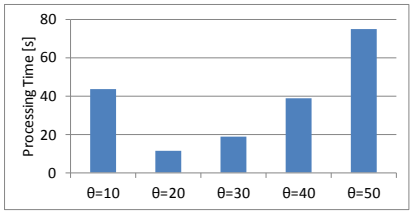

Figure 11: Processing Time for each θ.

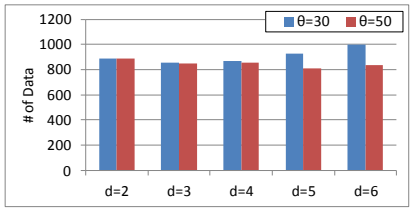

Figure 12: The number of records by θs.

to get the minimal number of records. However the best d depends on θ. The fact implies that both d and θ should be selected carefully to get the smallest sparse representation.

5 CONCLUSIONS

We proposed a method for managing quantity distributions. With this method, a sparse representation of a quantity distribution is derived using kernel ridge regression. The sparse representation dataset is small enough to handle by using RDBMSs without high cost. An advantage of the proposed method is that the reconstruction can be written in SQL. Therefore the proposed method can easily provide drill-down functions. We experimentally applied the algorithm of the proposed method to DEM data. As a result, the number of records was reduced to less than 1/10 (e.g. 3.9%) that of the original number. In addition, the data retrieval performance was comparable with that for the original dataset. This shows that the proposed method can reduce records without loss of speed.

SVR, of which formula is more sparse than that of kernel ridge regression, is also well known. A SVR-based sparse representation thus might be more compact. A reason why the algorithm of the proposed method uses kernel ridge regression is that the kernel ridge regression ensures accuracy if $\sigma = 0$. Support vector regression does not output such accurate representation; thus, an algorithm to generate an SVR-based sparse representation is for future work.

REFERENCES

Asahara, A., Hayashi, H., and Kai, T. (2015). Moving point density estimation algorithm based on a generated bayesian prior. *ISPRS International Journal of Geo-Information*, 4(2):515–534.

Bates, P. D. and De Roo, A. (2000). A simple raster-based model for flood inundation simulation. *Journal of hydrology*, 236(1):54–77.

Baumann, P., Dehmel, A., Furtado, P., Ritsch, R., and Widmann, N. (1999). Spatio-temporal retrieval with rasdaman. In *VLDB*, pages 746–749.

Christensen, J. H., Kjellström, E., Giorgi, F., Lenderink, G., Rummukainen, M., et al. (2010). Weight assignment in regional climate models. *Climate research (Open Access for articles 4 years old and older)*, 44(2):179.

David, H. D. and Thomas, K. P. (1973). Algorithms for the reduction of the number of points required to represent a hne or its caricature. *The Canadian Cartographer*, 10(2):112–122.

Hayashi, H., Asahara, A., Sugaya, N., Ogawa, Y., and Tomita, H. (2015). Spatio-temporal similarity search method for disaster estimation. In *2015 IEEE International Conference on Big Data (Big Data)*, pages 2462–2469. IEEE.

Haynes, D., Ray, S., Manson, S. M., and Soni, A. (2015). High performance analysis of big spatial data. In *2015 IEEE International Conference on Big Data (Big Data)*, pages 1953–1957. IEEE.

Hershberger, J. and Snoeyink, J. (1994). An o(nlogn) implementation of the douglas-peucker algorithm for line simplification. In *Proceedings of the Tenth Annual Symposium on Computational Geometry*, SCG '94, pages 383–384, New York, NY, USA. ACM.

Hofstra, N., Haylock, M., New, M., and Jones, P. D. (2009). Testing e-obs european high-resolution gridded data set of daily precipitation and surface temperature. *Journal of Geophysical Research: Atmospheres*, 114(D21).

International Standard Organization. ISO IEC CD 9075-15 Information technology – Database languages – SQL – Part 15: Multi dimensional arrays. http://www.iso.org/iso/home/store/catalogue_tc/catalogue_detail.htm?csnumber=67382.

John Shawe-Taylor, N. C. (2004). *Kernel Methods for Pattern Analysis*. Cambridge University Press.

Kbiob, D. (1951). A statistical approach to some basic mine valuation problems on the witwatersrand. *Journal of Chemical, Metallurgical, and Mining Society of South Africa*.

Koubarakis, M., Sellis, T., Frank, A. U., Grumbach, S., Güting, R. H., Jensen, C. S., Lorentzos, N., Manolopoulos, Y., Nardelli, E., Pernici, B., et al. (2003). *Spatio-temporal databases: The CHOROCHRONOS approach*, volume 2520. Springer.

Ministry of Land, Infrastructure, Transport and Turism (2014). National Land Numerical Information Data. http://nlftp.mlit.go.jp/ksj-e/index.html.

Open Geospatial Consortium (2010). OGC Network Common Data Form (NetCDF) Core Encoding Standard version 1.0 (10-090r3). http://www.opengeospatial.org/standards/netcdf.

Oracle (2014). Oracle Spatial and Graph GeoRaster, ORACLE WHITE PAPER SEPTEMBER 2014. http://download.oracle.com/otndocs/products/spatial/pdf/12c/oraspatialfeatures_12c_wp_georaster_wp.pdf.

Pajarola, R. and Widmayer, P. (1996). Spatial indexing into compressed raster images: how to answer range queries without decompression. In *Multimedia Database Management Systems, 1996., Proceedings of International Workshop on*, pages 94–100. IEEE.

Park, S., Bringi, V., Chandrasekar, V., Maki, M., and Iwanami, K. (2005). Correction of radar reflectivity and differential reflectivity for rain attenuation at x band. part i: Theoretical and empirical basis. *Journal of Atmospheric and Oceanic Technology*, 22(11):1621–1632.

Press, W. H., Teukolsky, S. A., Vetterling, W. T., and Flannery, B. P. (2007). *Numerical Recipes 3rd Edition: The Art of Scientific Computing*. Cambridge University Press, New York, NY, USA, 3 edition.

Seaman, D. E. and Powell, R. A. (1996). An evaluation of the accuracy of kernel density estimators for home range analysis. *Ecology*, 77(7):2075–2085.

Shyu, C.-R., Klaric, M., Scott, G. J., Barb, A. S., Davis, C. H., and Palaniappan, K. (2007). Geoiris: Geospatial information retrieval and indexing systemContent mining, semantics modeling, and complex queries. *IEEE Transactions on geoscience and remote sensing*, 45(4):839–852.

Silverman, B. W. (1986). *Density Estimation for Statistics and Data Analysis*. Chapman and Hall/CRC.

Stonebraker, M., Duggan, J., Battle, L., and Papaemmanouil, O. (2013). Scidb DBMS research at M.I.T. *IEEE Data Eng. Bull.*, 36(4):21–30.

the European Climate Assessment & Dataset project team (2016). European Climate Assessment & Dataset, Daily Data. http://www.ecad.eu/dailydata/index.php.

Theodoridis, Y., Sellis, T., Papadopoulos, A. N., and Manolopoulos, Y. (1998). Specifications for efficient indexing in spatiotemporal databases. In *Scientific and Statistical Database Management, 1998. Proceedings. Tenth International Conference on*, pages 123–132. IEEE.

Vapnik, V., Golowich, S. E., Smola, A., et al. (1997). Support vector method for function approximation, regression estimation, and signal processing. *Advances in neural information processing systems*, pages 281–287.

Zhang, J., You, S., and Gruenwald, L. (2010). Indexing large-scale raster geospatial data using massively parallel gpgpu computing. In *Proceedings of the 18th SIGSPATIAL International Conference on Advances in Geographic Information Systems*, pages 450–453, New York, NY, USA. ACM.